PHASE STABILITY TECHNIQUE FOR INVERSE SCATTERING IN OPTICAL COHERENCE TOMOGRAPHY

Tyler S. Ralston, Daniel L. Marks, P. Scott Carney, Stephen A. Boppart

University of Illinois at Urbana-Champaign,
Department of Electrical and Computer Engineering,
Beckman Institute for Advanced Science and Technology,

ABSTRACT

We present a technique for maintaining phase stability in a three-dimensional optical coherence tomography system. When determining the inverse scattering solution, phase stable measurements are required to ensure proper object reconstruction. The proposed method uses a reference object placed above the specimen to facilitate the retrieval of accurate constant phase surfaces throughout the specimen. Our algorithm locates the reference object, determines the phase and group delay, and corrects the phase disturbance accordingly.

1. INTRODUCTION

Optical microscopy has long relied on the design of physical optical elements to produce images of samples. However, with the advent of scanning modalities such as confocal microscopy, near-field scanning optical microscopy and optical coherence tomography (OCT), image quality is determined as much by algorithm development as the quality of optical elements. Data synthesis and image formation algorithms have been crucial in other non-optical imaging modalities such as synthetic aperture radar (SAR) where improved algorithms have dramatically increased the performance of such systems. For example, the modeling of physical parameters has lead to enhanced modes of strip-map and spotlight SAR imaging [1].

OCT is an optical ranging technique for mapping near-infrared backscattered light as it is scanned over a biological specimen [2]. In principle, the concept of OCT is similar to that of ultrasound except that that light rather than sound is backscattered. In OCT, optical hardware such as adaptive optics or axicon lenses has been utilized to increase the transverse resolution over a large range of depths in a specimen [3]. These optical techniques and hardware can help generate images with high transverse resolution over relatively large scanning depths. Dynamic focusing or focus tracking is useful for en face imaging with optical coherence microscopy (OCM) [2], or for cross-sectional imaging, where the tight focus is scanned in depth into the specimen [4]. Dynamic focusing techniques in a system design may require specific hardware modifications that can be difficult to control in real time. Some authors have designed algorithms that improve the axial resolution by compensating for the nonlinear dispersion between data in the temporal domain and the spatial domain [5]. Of these methods, some are used to correct for the limited bandwidth of the laser spectrum, while others correct for the dispersion induced by the optical system or the specimen. However, modeling of the physical processes has been limited to a one-dimensional quasi-monochromatic model [6]. These models do not take into account the relationship between data acquired at different transverse positions of the beam nor the finite transverse extent properties of the medium. Some have tried to correct for artifacts produced by refraction, sample positioning, and the scanning procedure [7]. Feng and Wang have detailed a theoretical model of OCT including a lens and heterodyning model [8].

Our goal has been to digitally reduce the distortion outside of the confocal region by solving the inverse problem based on the physics of the scattering process [9]. We have derived a mathematical model connecting the experimentally acquired OCT signal with the three-dimensional object structure, taking into account the finite beam width and focusing. Thus, we arrive at a solution to the inverse scattering problem (ISP), a transformation specifying the structure of an imaged object from the acquired data.

The increased resolution gained by the solution to the ISP relies upon phase stable measurements. Fortunately, with the use of spectral detection for OCT [10], spectral-domain OCT (SD-OCT) seen in Figure 1, we can be assured of phase stability within each axial data set. Specifically, each axial acquisition is determined directly from Fourier transform of the ensemble of spectral intensity measurements over the duration of the exposure time on a CCD camera. Thus, relative phases between adjacent reflections in the sample are fixed relative to each other and the reference for a single axial acquisition. Furthermore, if adjacent axial scans may be captured fast enough to avoid

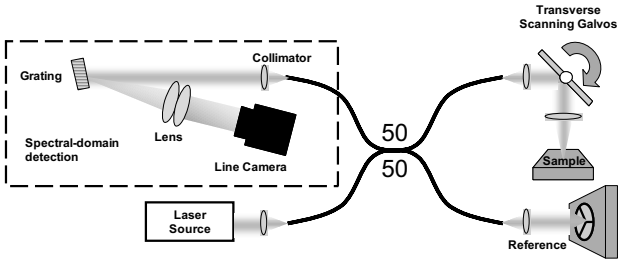

Fig. 1. A system diagram for spectral domain optical coherence tomography. The system is comprised of a broadband source, a fiber-based interferometer, and a spectral detector. Notice that data is collected at the camera as the optical Fourier transform.

some minimum amount of phase drift then an accurate reconstruction is possible. Phase drift can occur in a system for multiple reasons including thermal changes, galvanometer or stage positioning accuracy, and system or sample jitter. The greater the time interval between scans, the more likely random phase errors occur. Adjacent axial scans in a single cross-sectional scan are thus less likely to suffer from distortions due to random phase jitter than adjacent axial scans from multiple cross-sectional scans.

Object reconstruction requires the phase to be stable relative to all axial scans of a 3D acquisition. This paper shows a method to achieve 3D phase stability in OCT for reconstruction of the inverse scattering solution by using a flat reference reflector such as a microscope coverslip. Such a method offers advantages over expensive environmental controllers and extremely fast acquisition hardware.

2. OCT MODEL

2.1. Inverse scattering model

In order to simplify the model for OCT data acquisition several assumptions are generally made about an OCT system. These assumptions do not take into account the shape of wavefronts produced by lens optics, the spectrum of the source, or even unbalanced dispersion in the media. Thus, many OCT images exhibit poor transverse resolution outside of the confocal region, which manifest as curved and blurred features obtained in these areas. The aspect of the inverse problem this work addresses is the resolution of scatterers outside of the confocal region in experimental OCT data.

An equation for the acquired OCT signal

$$S(\mathbf{r}_0,k) = A(k)\int_{\Sigma} d^2r \int_{V} d^3r' G(\mathbf{r}',\mathbf{r},k)\, g(\mathbf{r}'-\mathbf{r}_0,k) \times g(\mathbf{r}-\mathbf{r}_0,k)\,\eta(\mathbf{r}')$$

is presented in terms of our model, see Fig. 2. This equation represents the linear forward problem having the form of a type I Fredholm integral. The adjoint and the normal operators can be diagonalized by a coordinate

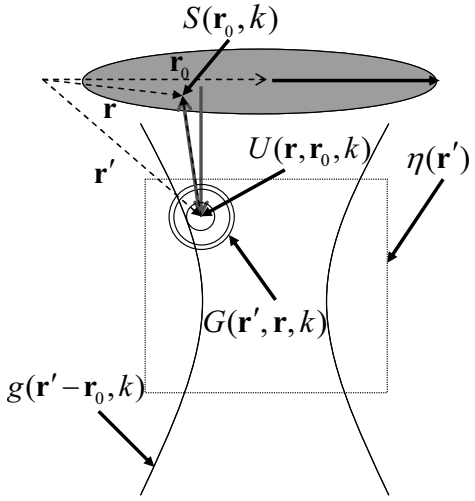

Fig. 2. The diagram of scattering from a Gaussian beam, where $\mathbf{r_0}$ is the transverse position of the beam, $G(\mathbf{r}',\mathbf{r},k)$ is the radiated Green's Function, $g(\mathbf{r}'-\mathbf{r_0},k)$ is the translated incident field with a Gaussian beam profile, and $\eta(\mathbf{r}')$ is the susceptibility of the object. The vector $\mathbf{r}'$ describes a point in the object volume, and the vector $\mathbf{r}$ describes points on the boundary of the volume.

transformation in the Fourier space such that a simplified least squares solution is formed. The pseudo inverse takes the following form, where $\mathbf{Q}$ is the Fourier transform coordinates of position $\mathbf{r_0}$.

$$\tilde{\tilde{\eta}}^{+}(\mathbf{Q};\beta) = F(\mathbf{Q},k)\tilde{S}(\mathbf{Q},k)\Big|_{k=\frac{1}{2}\left(\frac{\beta}{2}+\sqrt{\left(\frac{\beta}{2}\right)^2+\frac{Q^2}{2}}\right)},$$

where ~ denotes the Fourier transforms of η and S, and $F(\mathbf{Q},k)$ is a constant function of $\mathbf{Q}$ and k.

By solving the inverse problem, we are able to produce images with more sharply defined features. More importantly, we are able to distinguish closely adjacent scatterers, even those that produce interference in the raw OCT image. This is a crucial advantage of inverse scattering over simple deconvolution of a real-valued point-spread-function.

2.2. Phase model

The acquired SD-OCT signal can be represented after dispersion correction as a function of transverse position and wave number, $S(\mathbf{r_0},k)$, where the wave numbers k are related to the frequencies ω by the dispersion relation $k(\omega)=\omega\, n/c$, and n is the index of refraction.

We propose an algorithm that analyzes each axial scan individually and applies a phase to compensate variations of the position of the sample relative to the illumination beam. We place a reflective surface such as a microscope coverslip on top of the sample to act as a reference surface, which is used to infer the delay to the top surface of the sample. The

signal for an arbitrary axial line of data can be represented as $S(k)$, a function of k. We assume that there is a range of distances along the illumination beam $z_{\min}$ to $z_{\max}$ for which the signal reflected from the coverslip is known to reside in every axial scan. The inverse Fourier transform of $S(k)$ is computed as $S_c(z)$, and the signal corresponding to the reflection is contained in the samples $S_c(z)$ for $z_{\min} < z < z_{\max}$. The spatial spectrum of the reflection is computed as the Fourier transform of $S_c(z)$ over the window $z_{\min} < z < z_{\max}$, which is called $\tilde{S}_c(k)$.

Because the signal contained in $\tilde{S}_c(k)$ corresponds to a single reflection, it is reasonable to model it as $\tilde{S}_c(k) = A(k)e^{i\phi(k)}$, where the phase function $\phi(k) = \phi_0 + kd$, where ϕ_0 is an arbitrary phase and d is the true position of the surface where the reference reflection occurs. Because of the motion of the sample, the actual phase $\arg \tilde{S}_c(k) = \phi'(k)$. By multiplying the axial scan data $S(k)$ by the correction factor $e^{i[\phi(k)-\phi'(k)]}$, the phase of the axial scan can be adjusted to place the reflection at its true known position d.

We model the phase $\phi'(k)$, as a Taylor series around a center frequency k_0:

$$\phi'(k) = \phi'(k_0) + (k - k_0)\left.\frac{\partial \phi'}{\partial k}\right|_{k=k_0} + \ldots,$$

To utilize this model, we must estimate the value of $\partial\phi'/\partial k|_{k=k_0}$ from the data function $\phi'(k)$. The function $\phi'(k)$ is wrapped to the range $-\pi$ to π, so calculating the derivative directly from the wrapped data will incorrectly incorporate the 2π jumps into the estimate. Instead, we form the unwrapped $\phi_w(k)$ by removing 2π discontinuities from $\phi'(k)$. The estimate then becomes

$$\left.\frac{\partial \phi'}{\partial k}\right|_{k=k_0} \approx \frac{\phi_w(k_2) - \phi_w(k_1)}{k_2 - k_1}$$

where $k_1 < k_0 < k_2$, with the frequencies k_1 and k_2 chosen to span the illumination spectrum, typically with k_1 and k_2 corresponding to the frequencies at which the power spectral density is half of that at the peak.

Once $\phi'(k_0)$ and $\partial\phi'/\partial k|_{k=k_0}$ are known, the empirical $\phi'(k)$ can be computed, and the corrected axial scan spectrum $S'(k) = S(k)e^{i[\phi(k)-\phi(k')]}$. This corrected axial scan data will be modified such that the position of the reference reflection is always at the same location on the axial scan, removing the effective longitudinal relative motion between the sample and the scanned beam. For this method to work properly, the reference object must be located for each axial scan, otherwise that axial scan could contribute to a poor reconstruction. Furthermore, refinements to this method could utilize higher order terms of the series for $\phi'(k)$, which would account for instrument dispersion as well as motion.

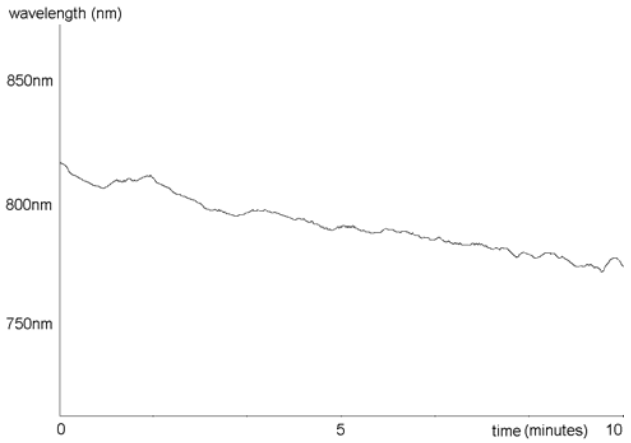

Fig. 3 Plot of wavelength (nm) verses time (minutes) of the constant phase fronts from a reflector in the SD-OCT system. This is a visual of the phase and group delay in the system over extended periods of time.

3. SYSTEM PHASE STABILITY

Tracking the phase in our system over a time of acquisition gives us an estimate of the amount of correction that will be needed. Figure 3 is a plot along isophase fronts of a reflector for a 10 minutes acquisition period. It can be seen that the phase drift is slowly varying, thus axial scans that occur close in time have more phase stability.

Our acquisition is done with a pair of galvanometers that scan in the x and y directions. The y galvanometer is incremented after each x scan, thus making y the slow scanning direction. Explicitly, each axial scan is acquired every 34 μs in the x direction, although in the y direction the adjacent axial scans can be delayed by 200 ms (at 5 frames per second) or more.

4. EXPERIMENT

A collection of scatterers having an average diameter of 2 μm were suspended in silicone and imaged with a spectral-domain OCT (SD-OCT) system. A volume of 800 μm X 800 μm (transverse) X 2000 μm (axial) was imaged, where the bandwidth is 100 nm, the focal length of the lens is 12 mm, the spot size is 9 μm, the confocal parameter is 636 μm, and the NA is 0.05. All images in the figures are planes at a constant value of the fast scan direction, where x is 164 μm from the edge (x = 0). Figure 4(a) displays a cross-sectional SD-OCT plane of the slow scanning direction. Drifting of the slide position in the z direction can be seen in the SD-OCT image. Figure 4(b) shows the plane

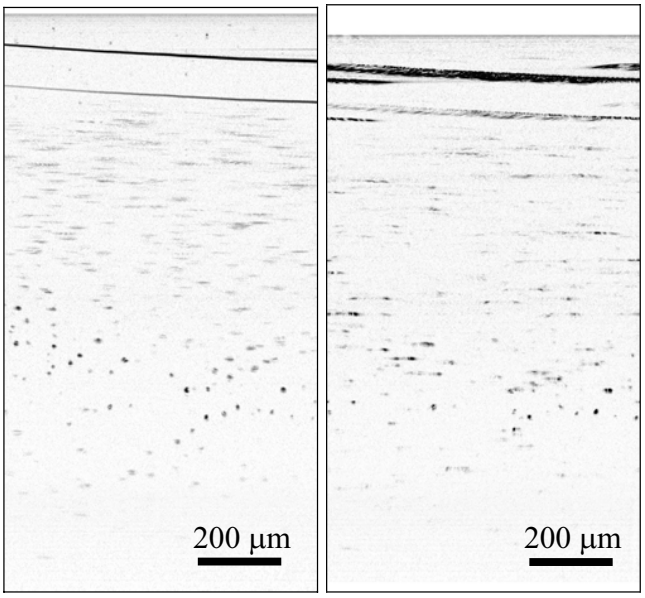

(a) (b)

Fig. 4.(a) Original cross-sectional SD-OCT image in the slow scanning direction after dispersion correction from a set of 3D data. (b) The same cross-sectional image after a 3D reconstruction, where the phase drift causes a poor reconstruction in the slow scanning direction.

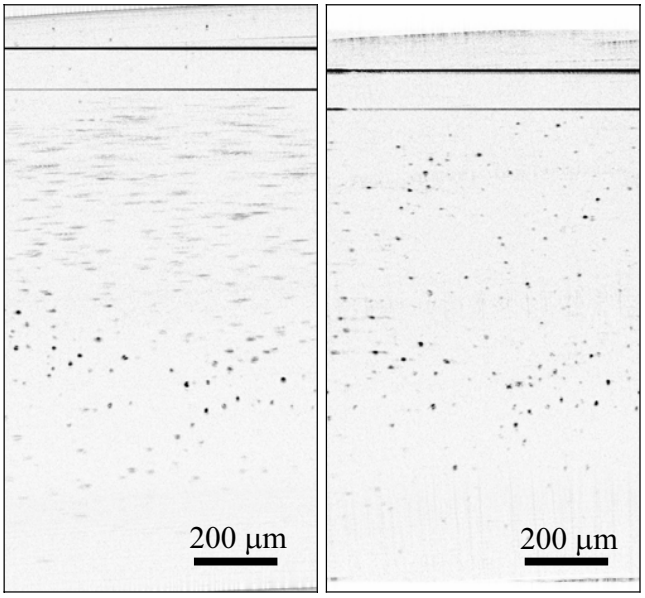

(a) (b)

Fig. 5.(a) A phase corrected cross-sectional SD-OCT image in the slow scanning direction after dispersion correction from a set of 3D data. (b) The same cross-sectional image after a 3D reconstruction, where the phase correction allows for an accurate reconstruction in the slow scanning direction.

after a 3D reconstruction. The resolution of point scatterers lying outside of the confocal region does not appear to be increased. This poor reconstruction is a result of this phase instability in the *y*, slow-scanning direction. Figure 5(a) displays the phase and group delay corrected SD-OCT plane. Figure 5(b) shows the plane after a 3D reconstruction. Notice that the scatterers are uniform size and appearance for all depths.

5. CONCLUSION

We have shown a method for maintaining phase stability in a three-dimensional OCT system, which is useful when determining the inverse scattering solution. It was shown that unstable phases result in an improper object reconstruction and that our method facilitates the retrieval of accurate constant phase surfaces throughout a specimen. By locating the reference object, determining the phase and group delay, and rephasing the data, the object can be reconstructed accurately.

6. REFERENCES

[1] P. S. Cooper, A. F. Wons, and A. P. Gaskell, "High resolution synthetic aperture radar using a multiple sub-band technique," *IEE Radar*, pp. 263-267, 1997.

[2] J. M. Schmitt, "Optical Coherence Tomography (OCT): A Review," *IEEE Journal of Selected Topics in Quantum Electronics*, vol. 5, pp. 1205-1215, 1999.

[3] Z. Ding, H. Ren, Y. Zhao, J. S. Nelson, and Z. Chen, "High-resolution optical coherence tomography over a large depth range with an axicon lens," *Optics Letters*, vol. 27, pp. 243-245, 2002.

[4] M. J. Cobb, X. Liu, and X. Li, "Continuous focus tracking for real-time optical coherence tomography," *Optics Letters*, vol. 30, pp. 1680-1682, 2005.

[5] M. D. Kulkarni, C. W. Thomas, and J. A. Izatt, "Image enhancement in optical coherence tomography using deconvolution," *Electronics Letters*, vol. 33, pp. 1365-1367, 1997.

[6] O. Bruno and J. Chaubell, "One-dimensional inverse scattering problem for optical coherence tomography," *Institute of Physics Publishing, Inverse problems*, pp. 499-524, 2005.

[7] A. Podoleanu, I. Charalambous, L. Plesea, A. Dogariu, and R. Rosen, "Correction of distortions in optical coherence tomography imaging of the eye," *Institute of Physics Publishing, Physics in Medicine and Biology*, pp. 1277-1294, 2004.

[8] Y. Feng and R. K. Wang, "Theoretical model of optical coherence tomography for system optimization and characterization," *Journal of the Optical Society of America*, vol. 20, pp. 1792-1803, 2003.

[9] T. Ralston, D. Marks, P. Carney, and S. Boppart, "Inverse Scattering for Optical Coherence Tomography," *Journal of Optical Society of America A*, in press.

[10] L. Lepetit, G. Cheriaux , and M. Joffre, "Linear techniques of phase measurement by femtosecond spectral interferometry for applications in spectroscopy," *Journal of Optical Society of America B*, vol. 12, pp. 2467-2474, 1995.